ACS APPLIED MATERIALS & INTERFACES

Forum Article

www.acsami.org

Hyper-Branched Phosphorescent Conjugated Polyelectrolytes for Time-Resolved Heparin Sensing

Huifang Shi,[†,‡] Xiujie,Chen[†,‡] Shujuan Liu,[†] Hang Xu,[†] Zhongfu An,[†] Lang Ouyang,[†] Zhenzhen Tu,[†] Qiang Zhao,*[,†] Quli Fan,[†] Lianhui Wang,[†] and Wei Huang*[,†,§]

[†]Key Laboratory for Organic Electronics & Information Displays (KLOEID), and Institute of Advanced Materials (IAM), Nanjing University of Posts and Telecommunications, Wenyuan Road 9, Nanjing 210023, China

[§]Jiangsu-Singapore Joint Research Center for Organic/Bio-Electronics & Information Displays and Institute of Advanced Materials, Nanjing University of Technology, Nanjing 211816, China

Supporting Information

ABSTRACT: A series of hyper-branched cationic conjugated polyelectrolytes containing different contents of phosphorescent Ir(III) complex has been designed and synthesized successfully. Their photophysical properties in both aqueous solution and solid film are investigated and their morphologies in aqueous solution are observed by TEM. Nanoparticles with the size of 80−100 nm have been formed in aqueous solution through the self-assembly of polymers. An energy transfer process from host polyfluorene to guest Ir(III) complex exists and becomes more efficient in the solid films. Importantly, this series of hyper-branched polymers can be applied as light-up heparin probes with good selectivity, high sensitivity, and naked-eye detection through electrostatic interaction between polymers and heparin. Quantification for heparin in aqueous solution can be realized in the range of 0−44 μM in the buffer solution. Detection limit can reach as low as 50 nM. More meaningfully, time-resolved photoluminescence technique is utilized successfully in the heparin sensing to eliminate the background fluorescence interference effectively and enhance the sensing sensitivity in the complicated media.

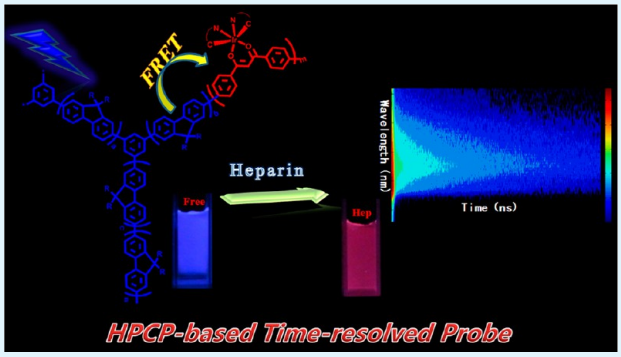

KEYWORDS: *conjugated polyelectrolytes, heparin probe, hyper-branched polymers, Ir(III) Complex, phosphorescence*

1. INTRODUCTION

Great efforts have been devoted to the conjugated polyelectrolytes (CPEs) for sensing and bioimaging in recent years.[1−6] Compared with the small-molecular organic dyes, the most attractive advantage for CPEs in sensing and bioimaging is their amplified signal output due to the "molecular wires" effect, which will enhance the sensing sensitivity significantly.[7] In addition, their good solubility in polar solvents, such as methanol or water, which will make the sensing in aqueous solution and in vitro/in vivo imaging feasible, endows CPEs ideal candidates in biosensing and bioimaging.[8−11] Hyper-branched conjugated polymers (HCPs) are a special type of dendritic polymers based on conjugated backbones with a feature of a high branching density in each repeating unit.[12] The highly branched molecular structures of HCPs can reduce the aggregation of CPEs in aqueous solution.[13] Moreover, HCPs also possess high photostability compared to their linear counterparts.[14] Hence, hyper-branched conjugated polyelectrolytes are very promising for sensing and bioimaging.

Although excellent sensing performances have been realized for CPEs, they are always interfered by the background fluorescence, which is derived from some organic dyes in the sensing media or from the biosamples themselves. Phosphorescent heavy metal complexes (PHMCs) with long emission lifetime can provide an effective means to resolve this problem by using time-resolved photoluminescence technique (TRPT).[15] Apart from the long emission lifetime, PHMCs exhibit some other merits, such as high quantum efficiency, good photostability, visible excitation, tunable emission color, and large Stokes shift.[16] Therefore, more and more attentions have been paid to the research of design and synthesis of phosphorescent probes based on heavy-metal complex,[17] such as Ir(III) complex, Ru(II) complex, Pt(II) complex, and so on. Among all these PHMCs, Ir(III) complex is considered as the most promising one due to its high quantum yield and rich ligand structures. Up to now, many excellent phosphorescent probes based on Ir(III) complex have been reported.[18,19]

Combining all the advantages of CPEs, HCPs, and PHMCs, it is quite interesting to introduce the phosphorescent Ir(III) complex into the hyper-branched conjugated polyelectro-

Special Issue: Forum on Conjugated Polymer Materials for Sensing and Biomedical Applications

Received: January 20, 2013
Accepted: March 7, 2013
Published: March 25, 2013

   dx.doi.org/10.1021/am4000408 | *ACS Appl. Mater. Interfaces* 2013, 5, 4562−4568

lytes.[20−22] In this contribution, we have designed and synthesized a series of hyper-branched phosphorescent conjugated polyelectrolytes (HPCPs) and investigated their application in biosensing. Herein, we choose heparin as an analyte, whose chemical structure is shown in Scheme 1.

Scheme 1. Chemical Structures of Heparin and Its Analogue HA

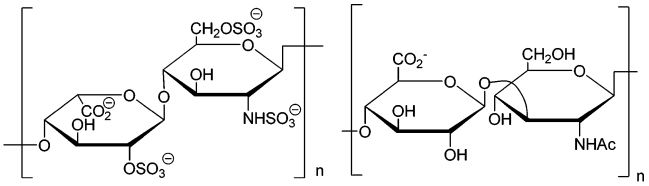

Heparin Hyaluronic acid (HA)

Heparin is one of the biomacromolecules with the most negative charged densities among all the known biomacromolecules, which can be used as a natural anticoagulant in the clinical applications. Heparin overdose, however, can cause serious problems, such as hemorrhage or thrombocytopenia.[23] Thus, it is quite meaningful to detect and quantify heparin. Up to now, there are many methods for heparin sensing, including traditional activated clotting time (ACT) and activated partial thromboplastin time (aPTT),[24] as well as fluorescent method.[25−32] Compared with the traditional techniques, the fluorescent method provides several unique advantages in terms of rapid response, low cost and high sensitivity. In this study, HPCP-based heparin probes with the switchable fluorescence and phosphorescence signal have been developed. A ratiometric probe for heparin quantification, naked-eye detection, and high sensitive sensing has been realized. Time-resolved emission spectra (TRES) have been utilized to eliminate the background fluorescence and enhance the signal-to-noise ratio of heparin sensing in the complicated media, demonstrating the advantages of phosphorescence signal in biosensing.

2. EXPERIMENTAL SECTION

2.1. Materials. All manipulations involving air-sensitive reagents were performed in an atmosphere of dry N_2 gas. $IrCl_3{\cdot}3H_2O$ was an industrial product and used without further purification. The solvents (THF and toluene) were purified by routine procedures and distilled under dry N_2 before use. Stock solutions for heparin (2 mM) and hyaluronic acid (HA) (2 mM) were prepared in Milli-Q water. Heparin molecular weight is calculated by the common repeat unit, which are 644.2 g/mol. Here the heparin has 170 U/mg and 1 μM is equal to 0.11 U/mg. The polymer concentrations were determined by the molecular weight of the repeat unit (RU), which was calculated through the feed ratios of the polymers. Stock solutions for polymers (1 mM) were prepared in methanol and diluted to different concentrations in 5 mM HEPES buffer aqueous solution. Rhodamine B (RB) (10 mM) was prepared in anhydrous ethyl alcohol.

2.2. Measurements. NMR spectra were obtained on Bruker Ultra Shield Plus 400 MHz instruments with tetramethylsilane as the internal standard. The UV−vis absorption spectra were measured on a UV-3600 Shimadzu UV−vis spectrophotometer. Transmission electron microscopy (TEM) was conducted on a JEOL JEM-2100 transmission electron microscope at an acceleration voltage of 150 kV. Mass spectra were recorded on a Bruker autoflex matrix-assisted laser desorption ionization time-of-flight (MALDI-TOF/TOF) mass spectrometer (MS3) and a Shimadzu GCMS-QP2010. The gel permeation chromatography (GPC) analysis of the polymers was conducted on a Shimadzu 10 Å with THF as the eluent and poly(styrene) as standard. The data were analyzed by the software package provided by Shimadzu Instruments. Photographs of the emission color in the solution were taken with a Cannon EOC 400D digital camera under a hand-held UV lamp. Photoluminescent spectra were measured on Edinburgh FL 920 instrument with Xe-lamp as an excitation source. TRES and emission lifetimes were obtained through a time-correlated single photon counting technique by the Edinburgh FL 920 instrument with a laser as the excitation source at 379 nm. Delayed photoluminescence spectra acquired after a 99 ns did not include the fluorescence from RB. Thus, the PL spectrum with a 99 ns delay was selected to compare with the total PL spectrum.

2.3. Synthesis of Polymers. The monomers (M_2, M_3 and M_4) were synthesized according to the previous reports.[33,34] All the polymers were prepared according to the same procedures, taking HPF-Ir2 as an example: the compounds M_1 (0.00975 mmol, 3.07 mg), M_2 (0.08135 mmol, 52.9 mg), M_3 (0.1 mmol, 74.4 mg), M_4 (0.0039 mmol, 3.9 mg), [$Pd(PPh_3)_4$] (5 mg) and tetrabutylammonium bromide (TBAB) were placed in a 25 mL round-bottomed flask. A mixed solvent of toluene (3 mL) and K_2CO_3 aqueous solution (2 mL, 2 M) were added .The reaction vessel was degassed and the reaction was stirred vigorously at 85 °C for 48 h under the protection of nitrogen-atmosphere. Then, the reaction was cooled down to RT and precipitated in methanol. The polymer was filtered and washed with methanol and acetone, and then dried under vacuum at RT for 24 h to obtain the polymer HPF-Ir2 precursor in the yield of 50%. Trimethylamine in tetrahydrofuran (1 mL, 2 mmol/L) was added dropwise to a solution of HPF-Ir2 precursor (40 mg) in THF (8 mL) at RT. The reaction was stirred at RT for 12 h. Then, the precipitate was redissolved by methanol (6 mL). Additional trimethylamine in tetrahydrofuran (1 mL, 2 mmol/L) was added, and the reaction was stirred at RT for 24 h. After removal of solvent, acetone was added to the precipitate. The polymer was dried under vacuum for 24 h to obtain the red solid (48 mg) with the yield of 87%.

HPF-Ir2 precursor. Yield: 53%. ^{1}H NMR (400 MHz, $CDCl_3$): δ 8.48 (d, 2% × 2H, Ar H of Ir complex), 8.04 (d, 2% × 2H, Ar H of Ir complex), 7.86−7.58 (m, 8H, Ar H of fluorene, Ir complex, and benzene), 6.41 (d, 2% × 2H, Ar H of Ir complex), 6.28 (s, 2% × 1H, CH of Ir complex), 3.31 (t, 4H, CH_2Br of fluorene), 2.15 (m, 4H, CH_2 of fluorene), 1.70 (m, 4H, CH_2 of fluorene), 1.44−1.18 (m, 8H, CH_2 of fluorene), 0.718 (m, 4H, CH_2 of fluorene). ^{13}C NMR (100 MHz, $CDCl_3$): δ 151.50, 140.53, 140.11, 135.79, 128.85, 128.26, 127.21, 126.38, 125.53, 121.33, 120.18, 67.99, 55.33, 40.30, 34.24, 34.01, 32.62, 30.34, 29.58, 29.07, 27.77, 25.63, 23.71, 21.20.

HPF-Ir4 precursor. Yield: 64%. ^{1}H NMR (400 MHz, $CDCl_3$): δ 8.48 (d, 3.6% × 2H, Ar H of Ir complex), 8.04 (d, 3.6% × 2H, Ar H of Ir complex), 7.85−7.50 (m, 8H, Ar H of fluorene, Ir complex, and benzene), 6.41 (d, 3.6% × 2H, Ar H of Ir complex), 6.27 (s, 3.6% × 1H, CH of Ir complex), 3.29 (t, 4H, CH_2Br of fluorene), 2.14 (m, 4H, CH_2 of fluorene), 1.68 (m, 4H, CH_2 of fluorene), 1.258−1.179 (m, 8H, CH_2 of fluorene), 0.727 (m, 4H, CH_2 of fluorene). ^{13}C NMR (100 MHz, $CDCl_3$): δ 151.50, 140.52, 140.13, 128.86, 127.22, 126.37, 121.33, 120.19, 55.33, 40.32, 34.03, 32.62, 29.08, 27.78, 23.70.

HPF-Ir8 precursor. Yield: 60%. ^{1}H NMR (400 MHz, $CDCl_3$): δ 8.49 (d, 7.8% × 2H, Ar H of Ir complex), 8.04 (d, 7.8% × 2H, Ar H of Ir complex), 7.85−7.39 (m, 8H, Ar H of fluorene, Ir complex and benzene), 6.42 (d, 7.8% × 2H, Ar H of Ir complex), 6.28 (s, 7.8% × 1H, CH of Ir complex), 3.29 (t, 4H, CH_2Br of fluorene), 2.15 (m, 4H, CH_2 of fluorene), 1.69 (m, 4H, CH_2 of fluorene), 1.265−1.18 (m, 8H, CH_2 of fluorene), 0.72 (m, 4H, CH_2 of fluorene). ^{13}C NMR (100 MHz, $CDCl_3$): δ 151.50, 140.52, 140.12, 128.86, 127.71, 126.78, 126.38, 121.34, 120.19, 55.33, 40.29, 34.02, 32.62, 29.71, 27.77, 23.71.

HPF-Ir2. Yield: 87%. ^{1}H NMR (400 MHz, CD_3OD): δ 8.48 (d, 2H), 8.04 (d, 2H), 7.91−7.36 (m, 8H), 6.41 (d, 2H), 6.28 (s, 1H), 3.28 (t, 4H), 3.05 (s, 17H), 2.23 (m, 4H), 1.59 (m, 4H), 1.27−1.17 (m, 8H), 0.765 (m, 4H). ^{13}C NMR (100 MHz, CD_3OD): δ 150.94, 144.39, 140.29, 129.53, 128.57, 126.03, 124.87, 120.91, 119.82, 66.31, 61.55, 60.49, 59.01, 55.43, 52.20, 40.25, 33.96, 29.89, 29.09, 28.47, 27.46, 25.48, 23.44, 22.35. Quarternization degree: 94%.

HPF-Ir4. Yield: 89%. ^{1}H NMR (400 MHz, CD_3OD): δ 8.48 (d, 2H), 8.04 (d, 2H), 7.92−7.38 (m, 8H), 6.41 (d, 2H), 6.27 (s, 1H), 3.30 (t, 4H), 3.05 (s, 16H), 2.21 (m, 4H), 1.61 (m, 4H), 139−1.19

dx.doi.org/10.1021/am4000408 | ACS Appl. Mater. Interfaces 2013, 5, 4562−4568

Scheme 2. Synthetic routes of the HPCPs

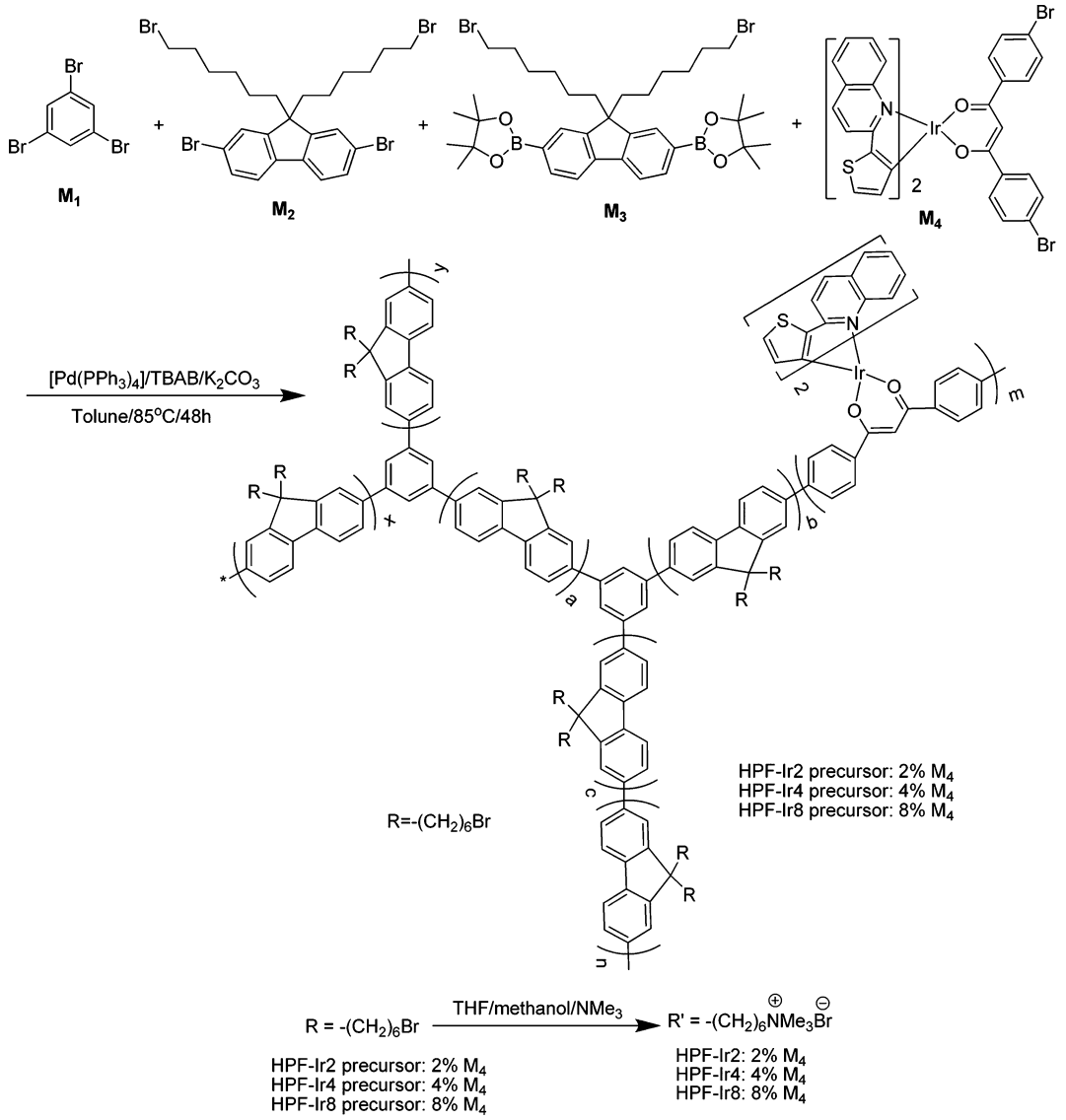

(m, 8H), 0.776 (m, 4H). ^{13}C NMR (100 MHz, CD_3OD): δ 151.30, 140.33, 128.72, 126.85, 125.95, 120.89, 66.31, 55.32, 52.21, 39.55, 33.38, 32.27, 29.44, 28.97, 27.09, 25.66, 22.42. Quarternization degree: 89%.

HPF-Ir8. Yield: 81%. ^{1}H NMR (400 MHz, CD_3OD): δ 8.48 (d, 2H), 8.04 (d, 2H), 7.94−7.36 (m, 8H), 6.42 (d, 2H), 6.26 (s, 1H), 3.30 (t, 4H), 3.05 (s,17H), 2.15 (m, 4H), 1.60 (m, 4H), 1.28−1.22 (m, 8H), 0.73 (m, 4H). ^{13}C NMR (100 MHz, CD_3OD): δ 151.32, 144.22, 140.36, 125.96, 120.69, 119.80, 97.26, 68.91, 66.42, 61.39, 59.18, 55.15, 52.20, 29.42, 28.48, 27.34, 25.67. Quarternization degree: 94%.

3. RESULTS AND DISCUSSION

3.1. Synthesis and Characterization. The synthetic routes of this series of HPCPs are shown in Scheme 2. The polymer precursors are prepared by Suzuki coupling reaction and the target HPCPs are obtained by the quarternization of the precursors. These polymers are characterized by ^{1}H NMR, ^{13}C NMR and GPC. These HPCPs are named as HPF-Ir2, HPF-Ir4, and HPF-Ir8 according to their feed ratios in the synthesis. It was found that the actual contents of Ir(III) complexes in the conjugated polymers were lower than those in the feed ratios probably caused by the difference of reaction activity and steric hindrance of Ir(III) complexes.[35] The weight-average molecular weights (M_w) of these HPCPs are estimated by GPC with the range from 51 000 to 57 000 and a polydispersity index (PDI) of 2.50−3.56 as shown in Table 1.

Table 1. Molecular Weight, Polydispersity Index, and Composition of the Polymers

				complex content (mol %)	
polymer	M_w	M_n	PDI	feed ratio	actual content
HPF-Ir2	54 300	15 300	3.55	2	2
HPF-Ir4	51 400	20 500	2.50	4	3.6
HPF-Ir8	57 500	17 750	3.24	8	7.8

The morphology of these HPCPs in aqueous solution was observed by TEM as shown in Figure 1. From the images, the nanoparticles (NPs) with the size of 80−100 nm were formed, which may be due to their amphiphilic and hyper-branched structures.

3.2. Photophysical Properties. The photophysical properties of the HPCPs were investigated and shown in Figure 2 and Table 2. The polymer concentrations are

dx.doi.org/10.1021/am4000408 | ACS Appl. Mater. Interfaces 2013, 5, 4562−4568

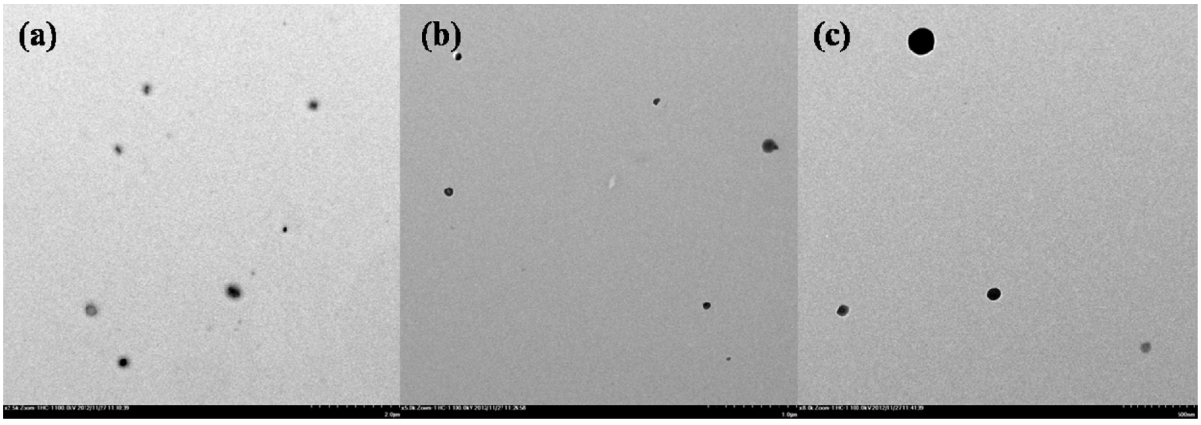

Figure 1. TEM images of (a) HPF-Ir2, (b) HPF-Ir4, and (c) HPF-Ir8 in aqueous solution.

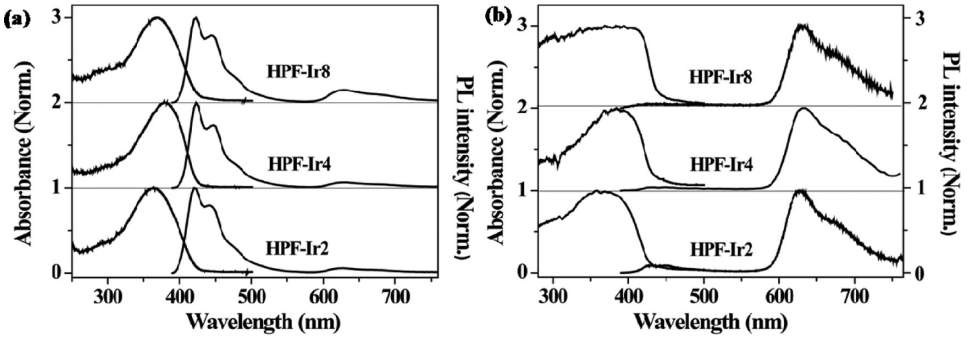

Figure 2. Absorption and PL spectra of HPCPs (a) in aqueous solution and (b) in film.

Table 2. Photophysical Properties of Conjugated Polymers

		UV (λ_{max}, nm)		PL (λ_{max}, nm)	
polymer	M_{RU} (g mol^{-1})	solution	film	solution	film
HPF-Ir2	588.4	365	365	420, 442, 628	429, 450, 628
HPF-Ir4	592.9	380	383	422, 445, 630	427,449, 633
HPF-Ir8	601.9	370	380	422, 445, 629	427, 448, 632

calculated using polymer repeat units (RU) based on the feed ratios. Figure 2a showed the absorption and PL spectra of the three polymers in aqueous solution. For the three polymers in aqueous solution (100 μM), a major absorption band lied in about 370 nm, which was assigned to the absorption of $\pi-\pi^*$ transitions of the polyfluorene unit. For PL spectra, a major emission peak at 420 nm with a shoulder at 445 nm was observed for three polymers. A weak emission peak at 630 nm assigned to Ir(III) complex was also observed, whose intensity enhanced with the increase of Ir(III)-complex content in the polymers. It indicated that the energy transfer from polyfluorene unit to Ir(III) complex became more efficient in the polymers with the higher Ir(III)-complex content. In film (Figure 2b), the major absorption band at about 380 nm and a weak band at 400−450 nm assigned to metal-to-ligand charge-transfer (MLCT) transition of the Ir(III) complex were observed for the HPCPs. For the PL spectra, the energy transfer became more efficient than that in solution. Even for HPF-Ir2, a strong phosphorescent emission peak at 630 nm with a weak blue emission peak was recorded. For HPF-Ir4 and HPF-Ir8, the blue emission at 420 nm almost disappeared and only the strong red emission from Ir(III) complex unit was observed.

3.3. Heparin Sensing. The quarternized side chains of the HPCPs made them positive charged in aqueous solution, which indicated that HPCPs can be used as heparin probe through electrostatic interaction. The content of Ir(III) complex in polymer should be optimized to achieve a significant spectral change upon heparin binding. The optimization experiments of heparin detection for the three target polymers were conducted in 5 mM buffer solution. For HPF-Ir2, with the low Ir(III)-complex content, there was no significant ratiometric spectral change before and after addition of heparin shown in Figure S1 in the Supporting Information (SI). And for HPF-Ir8, due to its high Ir(III)-complex content, the background red emission was quite obvious even before heparin addition, which suggested that a colorimetric detection of heparin in the aqueous solution cannot be realized efficiently (see Figure S2 in the Supporting Information). For HPF-Ir4, however, heparin-sensing in aqueous solution with both an evident ratiometric and colorimetric detection can be realized because of its proper Ir(III)-complex content in the polymer.[36]

As shown in Figure 3, heparin titration experiment was conducted at HPF-Ir4 concentration of 100 μM in 5 mM HEPES buffer solution at pH 7.4 (25 °C). In the absence of heparin, HPF-Ir4 showed a sharp blue emission peak at 425 nm and shoulders at 445 and 465 nm, and a weak red emission peak at 630 nm, due to an inefficient energy transfer from polymer host to Ir(III)-complex guest. The PL spectra changed with addition of heparin to the system. The blue emission decreased gradually and the red emission from Ir(III) complex lighted up, leading to a ratiometric detection. Meanwhile, the emission color changed significantly from blue to red, realizing a colorimetric and naked-eye detection for heparin (Figure 3 inset image). When the heparin concentration increased to 48

dx.doi.org/10.1021/am4000408 | ACS Appl. Mater. Interfaces 2013, 5, 4562−4568

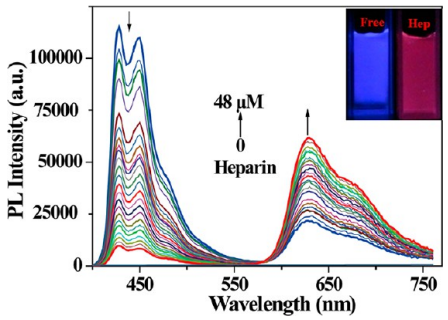

Figure 3. PL spectra of HPF-Ir4 at [RU] = 100 μM in 5 mM HEPES buffer with addition of heparin from 0 to 48 μM excited at 380 nm. Inset: emission color of the polymer solution in the absence and presence of heparin under hand-held UV-lamp excited at 365 nm.

μM, the heparin titration became balanced. Because of their electrostatic interaction between polymer probe and heparin, the titration reached charge balance.

Heparin quantification in the clinical application is very important. To quantify heparin detection for the HPCP-based probe, a parameter φ was defined as follows

$$\varphi = (I - I_0)/I_0$$

where I_0 means the PL spectral intensity of HPF-Ir4 at 630 nm in the absence of heparin and I is the PL intensity with different heparin concentrations. Φ as a function of heparin concentration together with its linear trendline was shown in Figure 4. A good linear relationship between heparin

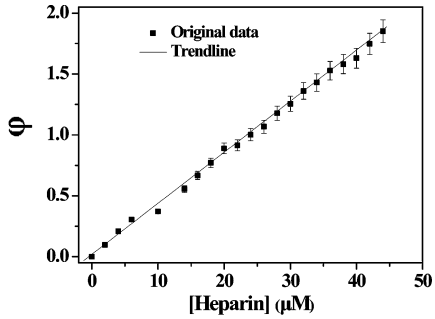

Figure 4. φ as a function of heparin concentration and its trendline at [RU] = 100 μM;.

concentrations in the solution and PL intensity changes was demonstrated, indicating that heparin quantification can be realized in the range of 0−44 μM in aqueous solution. In the clinical application, heparin concentration at the therapeutic dosing level is 0.2−8.0 U/mL (1.8−72.0 μM).[26,36] The heparin quantification range of HPCP-based probe is in the range of the therapeutic dosing level, which indicates that HPCP-based probe will be promising in the practical application.

For an excellent probe, high selectivity and sensitivity are two essential targets. Hyaluronic acid (HA), an analogue of heparin, as well as other three biomacromolecules in our lab, bovine serum albumin (BSA), hemoglobin (Hb) and lysozyme (Lys), was chosen to investigate the selectivity and competivity of the polymer probe. The experiments were conducted at HPF-Ir4 (100 μM) in 5 mM HEPES buffer. PL spectra were recorded for HPF-Ir4 with addition of different biomacromolecules (30 μM) and heparin (30 μM) containing other biomolecules, respectively (Figures S3−S6 in the Supporting Information). As shown in Figure 5, there was no evident red-emission light-up for polymer with addition of other biomolecules. HA, however,

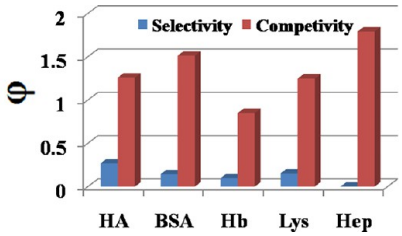

Figure 5. φ as a function of HPF-Ir4 in the presence of heparin and its analogue, HA, as well as some biomacromolecules. Hep, HA, BSA, Hb and Lys stand for heparin, hyaluronic acid, bovine serum albumin, hemoglobin and lysozyme, respectively.

can cause some spectral changes due to its quite similar structure with heparin and its negative-charged property. The red emission increased significantly for the polymer containing other biomacromolecules upon subsequent addition of heparin, which indicated that the polymer probe showed relative good competivity.

To study its sensitivity, the experiment of heparin titration was carried out in diluted polymer solution (4.5 μM). The PL spectra were recorded for HPF-Ir4 in 5 mM HEPES buffer solution with addition of heparin at the interval of 50 nM. As shown in Figure 6a, the blue emission decreased whereas the red emission increased gradually with titration of heparin. An evident PL spectral change was observed even with heparin concentration of 50 nM, which suggested that the limit of detection can be as low as 50 nM. From the linear trendline (Figure 6b), heparin quantification can be realized from 0 to 400 nM.

Moreover, the experiments for HPF-Ir4 in HEPES buffer containing 5% fatal bovine serum (FBS) with addition of heparin were also conducted as shown in Figure S7 in the Supporting Information. A clear PL spectra change was observed in the absence and presence of heparin, although an obvious red emission existed before addition of heparin due to the interaction between HPF-Ir4 and FBS itself. To prove the stability of the HPCP-based probe, the experiments for HPF-Ir4 (50 μM) with addition of NaCl in aqueous solution with different concentrations have been carried out. As shown in Figure S8 in the Supporting Information, there are almost no obvious changes for PL spectra of HPF-Ir4 with addition of different ion concentrations. However, the red emission increased clearly for HPF-Ir4 containing NaCl (100 mM) with addition of heparin, which indicated that the influence of ion concentration on the sensing performance is quite low because of the good water solubility for the polyelectrolyte.

In practical application, there are always background fluorescence interferences from the sensing media, which are often derived from some organic dyes and biosamples. As we known, the background fluorescence is often short-lived, but the red emission assigned to Ir(III) complex unit in the polymer probe is phosphorescent emission with long lifetime. Taking this unique advantage, time-resolved technique was applied to eliminate the background interference and enhance the sensing sensitivity.[37,38] RB was chosen as an example of background interference, which was dissolved in anhydrous ethanol. The TRES experiments were conducted at HPF-Ir4 (100 μM) in 5 mM HEPES buffer solution containing RB (30

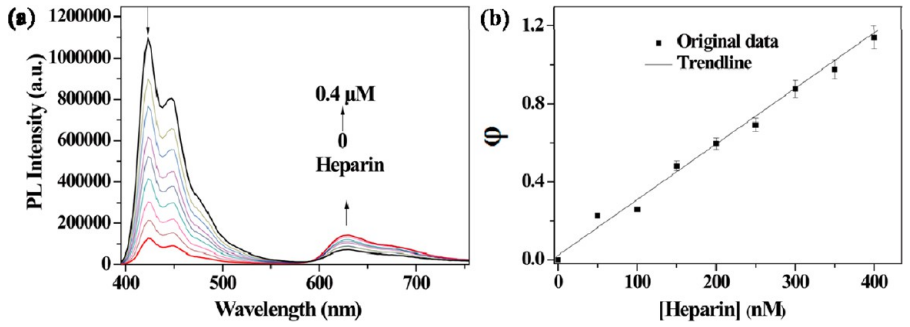

Figure 6. (a) PL spectra of HPF-Ir4 in 5 mM HEPES buffer at [RU] = 4.5 μM with addition of heparin; (b) φ as a function of heparin concentration and its trendline at [RU] = 4.5 μM.

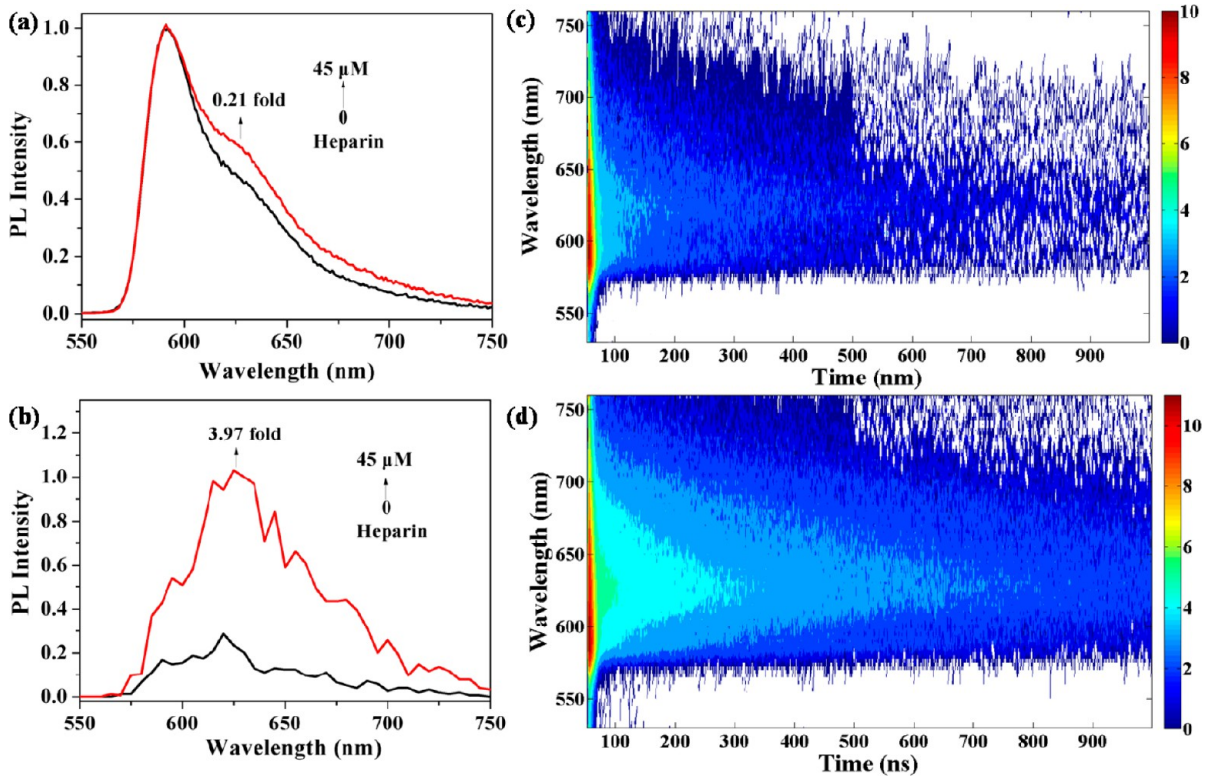

Figure 7. PL spectra of HPF-Ir4/RB mixture in 5 mM HEPES buffer with addition of heparin (a) in a steady state and (b) at delayed time of 99 ns. TRES at room temperature (excited at 379 nm) of HPF-Ir4/RB in the absence (c) and presence (d) of heparin (45 μM).

μM) with addition of heparin (45 μM). As shown in Figure 7a, in the steady state, there almost no light up for the PL spectra at 630 nm of HPF-Ir4 containing RB with addition of heparin. And only an intense emission at 590 nm was observed, which was attributed to RB. It suggested that there was strong fluorescent interference from RB for the heparin sensing. After 99 ns delay, however, the red emission at 630 nm increased by about 4-fold for HPF-Ir4 upon addition of heparin in the presence of RB (Figure 7b). And the TRES at room temperature showed significant spectral changes of HPF-Ir4 in the absence and presence of heparin (Figure 7c, d). These results indicated that the short-lived background fluorescence from RB can be eliminated effectively by using TRPT, which has proved that our phosphorescent hyper-branched polymer probe will be very promising in the practical applications.

CONCLUSIONS

In summary, we have developed a series of hyper-branched phosphorescent conjugated polyelectrolytes and their applications in heparin sensing. These hyper-branched polymers show good solubility in polar solvent. Energy transfer becomes more efficient for all the polyelectrolytes in film than that in solution. Polymer nanoparticles with the sizes around 100 nm are formed in the aqueous solution due to their amphiphilic structures. Because of its proper Ir(III)-complex content in the polymer, HPF-Ir4 can be utilized as a ratiometric and colorimetric heparin probe with high selectivity and low detection limit. Heparin quantification can be realized in the range of 0−44 μM. More importantly, taking advantage of long emission lifetime of the polymer, TRES is applied in the heparin sensing in the complicated media. The background fluorescence interference is eliminated by exerting the time delay between photoexcitation and acquisition of signals, and the signal-to-noise ratio of sensing is enhanced significantly.

dx.doi.org/10.1021/am4000408 | ACS Appl. Mater. Interfaces 2013, 5, 4562−4568

Thus, this probe will be a valuable tool for exploring time-resolved sensing system in the complicated media and be very promising in the practical applications.

■ ASSOCIATED CONTENT

Supporting Information

PL spectra of HPF-Ir2 and HPF-Ir8 in aqueous solution with addition of heparin, PL spectral data for selectivity and competivity. This material is available free of charge via the Internet at http://pubs.acs.org.

■ AUTHOR INFORMATION

Corresponding Author

*Tel: +86 25 5813 9988. Fax: +86 25 5813 9001. E-mail: iamwhuang@njupt.edu.cn (W.H.); iamqzhao@njupt.edu.cn (Q.Z.).

Author Contributions

‡H.S. and X.C. contributed equally to this work.

Notes

The authors declare no competing financial interest.

■ ACKNOWLEDGMENTS

We thank the National Basic Research Program of China (973 Program, 2009CB930601 and 2012CB933301), National Natural Science Foundation of China (Project 61274018, 21174064, 21171098), and the Ministry of Education of China (IRT1148), Key Projects in Jiangsu Province for International Cooperation (BZ2010043), Natural Science Foundation of Jiangsu Province of China (BK2012835), and Priority Academic Program Development of Jiangsu Higher Education Institutions.

■ REFERENCES

(1) Jiang, H.; Taranekar, P.; Reynolds, J. R.; Schanze, K. S. *Angew Chem., Int. Ed.* **2009**, *48*, 4300−4316.

(2) Liu, B.; Bazan, G. C. *Chem. Mater.* **2004**, *16*, 4467−4476.

(3) Feng, X. L.; Liu, L. B.; Wang, S.; Zhu, D. B. *Chem. Soc. Rev.* **2010**, *39*, 2411−2419.

(4) Zhu, C. L.; Liu, L. B.; Yang, Q.; Lv, F. T.; Wang, S. *Chem. Rev.* **2012**, *112*, 4687−4735.

(5) Yang, Q.; Dong, Y.; Wu, W.; Zhu, C. L.; Chong, H.; Lu, J. Y.; Yu, D. H.; Liu, L. B.; L, F. T.; Wang, S.. *Nat. Comm.* **2012**, *3*, 1206−1213.

(6) Ji, X. F.; Yao, Y.; Li, J. Y.; Yan, X. Z.; Huang, F. H. *J. Am. Chem. Soc.* **2013**, *135*, 74−77.

(7) Duarte, A.; Pu, K. Y.; Liu, B.; Bazan, G. C. *Chem. Mater.* **2011**, *23*, 501−515.

(8) Wu, C. F.; Jin, Y. H.; Schneider, T.; Burnham, D. R.; Smith, P. B.; Chiu, D. T. *Angew. Chem., Int. Ed.* **2010**, *49*, 9436−9440.

(9) Lee, K.; Lee, J.; Jeong, J. E.; Kronk, A.; Elenitoba-Johnson, K. S. J.; Lim, M. S.; Kim, J. *Adv. Mater.* **2012**, *24*, 2479−2484.

(10) Liu, J.; Geng, J. L.; Liu, B. *Chem. Commun.* **2013**, *49*, 1491−1493.

(11) Feng, X. L.; Lv, F. T.; Liu, L. B.; Yang, Q.; Wang, S.; Bazan, G. C. *Adv. Mater.* **2012**, *24*, 5428−5432.

(12) Voit, B. I.; Lederer, A. *Chem. Rev.* **2009**, *109*, 5924−5973.

(13) Bao, B. Q.; Yuwen, L. H.; Zhan, X. W.; Wang, L. H. *J. Polym. Sci., Part A: Polym. Chem.* **2010**, *48*, 3431−3439.

(14) Pu, K. Y.; Li, K.; Shi, J. B.; Liu, B. *Chem. Mater.* **2009**, *21*, 3816−3822.

(15) You, Y.; Lee, S.; Kim, T.; Ohkubo, K.; Chae, W. S.; Fukuzumi, S.; Jhon, G. J.; Nam, W.; Lippard, S. J. *J. Am. Chem. Soc.* **2011**, *133*, 18328−18342.

(16) Zhao, Q.; Huang, C. H.; Li, F. Y. *Chem. Soc. Rev.* **2011**, *40*, 2508−2524.

(17) Zhao, Q.; Li, F. Y.; Huang, C. H. *Chem. Soc. Rev.* **2010**, *39*, 3007−3030.

(18) Ma, Y.; Liu, S. J.; Yang, H. R.; Wu, Y. Q.; Yang, C. J.; Liu, X. M.; Zhao, Q.; Li, F. Y.; Huang, W. *J. Mater. Chem.* **2011**, *21*, 18974−18982.

(19) Chung, C. Y.; Yam, V. W. W. *J. Am. Chem. Soc.* **2011**, *133*, 18775−18784.

(20) Zhao, Q.; Liu, S. J.; Huang, W. *Macromol. Rapid Commun.* **2010**, *31*, 794−807.

(21) Liu, S. J.; Zhao, Q.; Mi, B. X.; Huang, W. *Adv. Polym. Sci.* **2008**, *212*, 125−144.

(22) Liu, S. J.; Chen, Y.; Xu, W. J.; Zhao, Q.; Huang, W. *Macromol. Rapid Commun.* **2012**, *33*, 461−480.

(23) Zhan, R. Y.; Fang, Z.; Liu, B. *Anal. Chem.* **2010**, *82*, 1326−1333.

(24) Nader, H. B.; Chavante, S. F.; Santos, E. A.; Oliveira, F. W.; Paiva, J. F.; Jeronimo, S. M.; Medeiros, G. F.; Abreu, L. R.; Leite, E. L.; Sousa, J. F.; Castro, R. A.; Toma, T.; Tersariol, I. L.; Porcionatto, M. A.; Dietrich, C. P. *Braz. J. Med. Biol. Res.* **1999**, *32*, 529−538.

(25) Pu, K. Y.; Zhan, R. Y.; Liang, J.; Liu, B. *Sci. China−Chem.* **2011**, *54*, 567−574.

(26) Pu, K. Y.; Liu, B. *Adv. Funct. Mater.* **2009**, *19*, 277−284.

(27) Jagt, R. B.; Gomez-Biagi, R. F.; Nitz, M. *Angew. Chem., Int. Ed.* **2009**, *48*, 1995−1997.

(28) Yeung, M. C.; Yam, V. W. W. *Chem.—Eur. J.* **2011**, *17*, 11987−11990.

(29) Cai, L. P.; Zhan, R. Y.; Pu, K. Y.; Qi, X. Y.; Zhang, H.; Huang, W.; Liu, B. *Anal. Chem.* **2011**, *83*, 7849−785.

(30) Jagt, R. B.; Gomez-Biagi, R. F.; Nitz, M. *Angew. Chem., Int. Ed.* **2009**, *48*, 1995−1997.

(31) Wang, S. L.; Chang, Y. T. *Chem. Commun.* **2008**, 1173−1175.

(32) Dai, Q.; Liu, W. M.; Zhuang, X. Q.; Wu, J. S.; Zhang, H. Y.; Wang, P. F. *Anal. Chem.* **2011**, *83*, 6559−6564.

(33) Shi, H. F.; Liu, S. J.; Sun, H. B.; Xu, W. J.; An, Z. F.; Chen, J.; Sun, S.; Lu, X. M.; Zhao, Q.; Huang, W. *Chem.—Eur. J.* **2010**, *16*, 12158−12167.

(34) Liu, B.; Bazan, G. C. *Nat. Prot.* **2006**, *1*, 1698−1702.

(35) Liu, S. J.; Zhao, Q.; Chen, R. F.; Deng, Y.; Fan, Q. L.; Li, F. Y.; Wang, L. H.; Huang, C. H.; Huang, W. *Chem.—Eur. J.* **2006**, *12*, 4351−4361.

(36) Shi, H. F.; Sun, H. B.; Yang, H. R.; Liu, S. J.; Jenkins, G.; Feng, W.; Li, F. Y.; Zhao, Q.; Liu, B.; Huang, W. *Adv. Funct. Mater.* **2013**, DOI: 10.1002/adfm.201202385, published online Feb 6th, 2013

(37) Liu, S. J.; Sun, H. B.; Ma, Y.; Ye, S. H.; Liu, X. M.; Zhou, X. H.; Mou, X.; Wang, L. H.; Zhao, Q.; Huang, W. *J. Mater. Chem.* **2012**, *22*, 22167−22173.

(38) Tang, Y.; Yang, H. R.; Sun, H. B.; Liu, S. J.; Wang, J. X.; Zhao, Q.; Liu, X. M.; Xu, W. J.; Li, S. B.; Huang, W. *Chem.—Eur. J.* **2013**, *4*, 1311−1319.